

## Chapter 5

### Nucleosynthesis in Supernovae

The explosion of a core-collapse supernova leads to ejection of the star's mantle, and thus to substantial enrichment of the interstellar medium with the major burning products of hydrostatic equilibrium:  ${}^4\text{He}$ ,  ${}^{12}\text{C}$ ,  ${}^{16}\text{O}$ ,  ${}^{20}\text{Ne}$ , etc. As was described in the first lecture of this course, these are among the most plentiful elements in nature. However neither this mechanism nor any other process we have discussed so far describes how many other elements found in nature are synthesized. In this chapter several mechanisms associated with the explosive conditions of a supernova - explosive nucleosynthesis, the s- and r-processes, and the neutrino process - will be described.

#### 5.1 Explosive nucleosynthesis and the iron peak

The creation of elements by the explosion itself - e.g., the high temperatures associated with passage of the shock wave - is called explosive nucleosynthesis. The properties of this process are tied to those of the explosion, which we have seen are still poorly understood. But the observation that the kinetic energy of a supernova explosion is typically in the range of  $(1-4) \cdot 10^{51}$  ergs, provides an important constraint.

Estimates of this synthesis depend on a number of issues:

- Description of the presupernova model. The conventional approach is to evolve a star of given initial composition (e.g., metal content) through the various burning stages. The result is influenced by the assumed initial metallicity, the nuclear cross sections adopted, and the physical mechanisms modeled, such as mass loss and convection.
- The galactic model. Presumably the abundances we see today result from integrating over a large number of events. Thus one needs to know the characteristics of typical supernovae, e.g., the distribution of Type II supernovae over possible masses. And one has to take account of evolutionary effects: are the number of large stars in the early history of our galaxy

similar to today? How does the supernova rate evolve? Was there an early “bright phase” in our galaxy’s evolution? Do overall changes in our galaxy, such as its metallicity, have an effect on supernova characteristics?

- Reaction rates. Our information about exotic nuclear reactions - reactions involving excited states, unstable nuclei that have not been studied in the laboratory, or simply reactions that have not been measured - often is too limited. Thus there is always some change being made due to new information from laboratory measurements.

For a mass point well away from the neutrinosphere - perhaps 30,000 kilometers from the center of the star - it is a reasonable approximation to assume the density and temperature of the matter are changed little during the explosion until the shock wave arrives at that point. There is an approximate expression for the time of shock arrival

$$t_0 \sim 0.7r_9 \sqrt{\frac{M_r - M_{NS}}{E_{51}}} \text{ s}$$

where  $r_9$  is the radius of point in  $10^9$  km,  $E_{51}$  is the energy of the explosion in  $10^{51}$  ergs,  $M_{NS} \sim 1.4$  solar masses is the mass of the newly formed neutron star, and  $M_r$  is the Lagrangian mass coordinate of the shell in question. Under the assumption that the part of the supernova behind the shock front is approximately isothermal and that the energy is contained in the radiation field, one might expect the peak temperature  $T_p$  produced by the shock wave to be

$$T_p^4 \cdot \frac{4\pi a r_o^3}{3} = E$$

where  $a$  is the radiation constant ( $a = 7.56 \times 10^{-15}$  ergs/cm<sup>3</sup>K<sup>4</sup> and is related to the Stefan Boltzmann constant by  $\sigma = ac/4$ ). The equation above says that the energy density of radiation ( $aT^4$ ) times the volume gives the explosion energy. Numerically a relation is obtained that is quite compatible with this simple picture

$$T_p \sim 2.4 \times 10^9 E_{51}^{1/4} r_9^{-3/4}$$

For a 20 solar mass star (from Woosley et al.) one gets the following results

<i>Shell</i>	<i>Radius</i>	<i>T</i>	<i>T<sub>p</sub></i>	<i>Density</i>	<i>Mass</i>	<i>t<sub>shock</sub></i>
	( <i>cm</i> )	( <i>K</i> )	( <i>K</i> )	( <i>g/cm<sup>3</sup></i> )	( <i>solar</i> )	( <i>s</i> )
<i>hydrogen</i>	1.00E11	8.00E6	7.59E7	1.0E-2	6.26	154.3
<i>helium</i>	1.51E10	1.02E8	3.13E8	5.57E1	4.79	19.46
<i>carbon</i>	3.44E9	3.68E8	9.50E8	4.93E3	3.54	3.52
<i>neon</i>	1.78E9	7.56E8	1.56E9	3.28E4	2.73	1.44
<i>oxygen</i>	4.33E8	2.11E9	4.50E9	8.41E5	1.79	0.19
<i>silicon</i>	2.89E8	2.88E9	6.09E9	2.08E6	1.65	0.10

The numerical values are for the centers of each shell except for carbon, where the values are for the inner part of that shell. The difference between  $T_{peak}$  and  $T$  shows the elevated temperature that results from shock wave passage.

Note that  $T_p$  reaches several in units of  $T_9$  in the inner (silicon, oxygen, neon) shells. The resulting soup of photons,  $\alpha$ s, and nucleons of several hundred keV can clearly process material in these shells. In the silicon shell significant production of iron-peak elements results:  $^{56,57}\text{Fe}$ ,  $^{59}\text{Co}$ ,  $^{58,60,61,62}\text{Ni}$ ,  $^{63,65}\text{Cu}$ ,  $^{64,66}\text{Zn}$ . Other important productions includes  $^{44}\text{Ca}$ ,  $^{48}\text{Ti}$ , etc. The pattern is quite similar in the oxygen shell. The somewhat lower  $T_p$  characterizing the neon shell shifts the synthesis to somewhat lighter nuclei, e.g.,  $^{28}\text{Si}$ ,  $^{32}\text{S}$ ,  $^{36}\text{Ar}$ ,  $^{41}\text{K}$ ,  $^{40,42}\text{Ca}$ , etc. Note many of these species can be formed by  $\alpha$  capture reactions that are facilitated by the higher temperatures. Outside the neon shell, very little explosive synthesis occurs.

It is quite possible that individual regions of the ejected mantle may remain more or less intact on ejection, thereby allowing observers to study the processes that occurred in each shell individually. Around 300-year-old supernova remnant Cas A regions have been found that are strongly overabundant in elements such as S, Ar, and Ca. Another exciting possibility - discussed in a recent Science magazine article - is to use the composition of individual stellar

grains to determine not only the conditions under which specific isotopes are synthesized, but also the specific chemistry connected with the ejection and cooling of the material from which these grains condensed.

## 5.2 Abundances above the iron peak and neutron capture

The figure shows the abundance pattern found in our solar system. We see abundant light nuclei, especially the H,  $^4\text{He}$ , and light elements. An abundance peak near the iron isotopes is seen. Then there are lower abundances for heavier isotopes, but also interesting structure: mass peaks are seen around  $A \sim 130$  and  $\sim 190$ . The low-mass structure (at and below iron) reflects a general tendency for Coulomb barriers to inhibit synthesis of increasingly heavier nuclei, with the iron group being exceptional because it is favored by its strong binding.

A blowup of the pattern of heavy elements shows a clear structure associated with the closed neutron shells in nuclear physics: the stablest configurations are at the closed shells  $N = 50$ ,  $82$ , and  $126$ . There is a splitting of the abundance peaks, suggesting that perhaps there are two processes of interest. One can also see that the integrated abundance above the iron peak is not large, comparable to about 3% of the iron peak. Thus the processes responsible can be reasonably rare.

This synthesis is associated with the neutron-capture reaction  $(n, \gamma)$ . There are sources of neutrons in stellar interiors, and neutron capture cross sections on heavy nuclei can be quite large. We will also see that the observed shell structure is natural for such a process. Unstable but long-lived neutron-capture products, such as technetium, are seen in the atmospheres of red giants, indicating that neutron-induced synthesis is occurring in the cores of existing stars (and then dredged up to the surface).

The nuclear physics for neutron capture follows directly from our earlier work on charged particle reactions, if we set the charge of the initiating particle to zero. Recall for the

compound nuclear reaction  $\alpha \rightarrow \beta$

$$\sigma_{\alpha\beta} = \frac{\pi}{k^2} \frac{\Gamma_\beta \Gamma_\alpha}{(E - E_r)^2 + (\frac{\Gamma}{2})^2}$$

where

$$\Gamma_\alpha \propto v P_l |\chi_l(R_N)|^2 \rightarrow \text{constant} \times v$$

for neutrons. It follows that

$$\sigma_{n\gamma} \propto 1/v \propto E^{-1/2}$$

Therefore

$$\langle \sigma v \rangle \sim \text{constant}$$

Since this quantity is independent of energy

$$r_{n1} = N_n N_1 \langle v \sigma \rangle \propto N_n N_1$$

The conclusion from these considerations is that the thermally averaged rate  $\langle \sigma v \rangle$  should depend on energy only implicitly through the nuclear structure: the result would be given by the average  $(n, \gamma)$  cross section times the density of such resonances near threshold. Such an average cross section is shown in the figure. Its dominant feature is the dips that occur at the closed neutron shells  $N = 8, 20, 28, 50, 82,$  and  $126$ . This reflects the very low level density in the vicinity of the closed shells: the shell gaps produce a low  $(n, \gamma)$  cross section.

### 5.3 The s-process

The s- and r-processes are mechanisms for synthesizing heavy nuclei by capturing neutrons one at a time. We consider the s-process first.

The following diagram of the  $(N, Z)$  plane shows the process of neutron capture in a plasma containing neutrons and heavy seed nuclei. The assumption made is that the neutron capture rate is much slower than the typical  $\beta$  decay rate, which then has several consequences:

- 1) The weak interactions are then fast and maintain the Z-N equilibrium: Every time a neutron is captured, the resulting system of A+1 nucleons has an opportunity to  $\beta$  decay to a nucleus of greater stability, if such a nucleus exists.
- 2) The rate of synthesis is then proportional to the rate of neutron capture: this controls the “mass flow” to heavier nuclei.
- 3) The path of nucleosynthesis, due to point 1) above, is thus along the so-called “valley-of-stability.” These are the familiar nuclei we study in laboratories, about which we know a great deal.

One consequence of the mass flow along the valley of stability is that a number of stable nuclei are avoided. One common situation is illustrated in the figure: frequently nuclei (N,Z) and (N+2,Z-2), when N and Z are even, are stable to  $\beta$  decay, while the odd-odd nucleus (N+1,Z-1) is unstable. The odd-odd nucleus has an unpaired proton and an unpaired neutron, accounting for its unfavorable ground state energy. The (N+2,Z-2) nucleus can be “shielded” from production in the s-process, as illustrated in the figure. Thus the existence of such isotopes with significant abundances indicates a second process, other than the slow- or s-process, must also occur.

One can also quantify the “slowness” of the s-process.  $\beta$  decay rates along the valley of stability are in the range of seconds to years. If one takes an average  $(n, \gamma)$  cross section of 0.1b at 30 KeV (corresponding to a neutron velocity of 0.008c), the reaction rate per particle pair is

$$\langle \sigma v \rangle = 2.4 \times 10^{-17} \text{cm}^3 \text{s}^{-1}$$

and the capture rate per heavy nucleus is obtained by multiplying this by the neutron number density. Thus if we require

$$\tau_{(n,\gamma)} \gtrsim 10\text{y} \Rightarrow N_n \lesssim 1.3 \cdot 10^8 \text{neutrons/cm}^3$$

Such a neutron density, if maintained for 2000 years, could synthesize  $A \sim 200$  nuclei from iron group seeds.

One can also offer arguments to place a lower bound on the required neutron density. No stable nucleus exists at  $N=61$ : there is, however, a long-lived isotope  $^{107}\text{Pd}$  with  $\tau_{1/2} \sim 7 \times 10^6$  y. Thus if the neutron capture rate is too slow,  $^{107}\text{Pd}$  will decay to  $^{107}\text{Ag}$ , and neutron capture will then produce the stable nucleus  $^{108}\text{Ag}$ . The nucleus  $^{108}\text{Pd}$  will be bypassed. This nucleus cannot be made in the r-process (to be discussed below) because  $^{108}\text{Pd}$  is shielded on the neutron-rich side by the stable nucleus  $^{108}\text{Cd}$ . We conclude that neutron capture must be fast enough to synthesize  $^{107}\text{Pd}$  in the s-process,

$$N_n \gtrsim 10^2 \text{neutrons/cm}^3$$

This neutron number density then permits  $^{108}\text{Pd}$  to be produced by guaranteeing neutron capture is faster than the  $\beta$  decay in this case.

The general equation describing the mass flow in the s-process is

$$\frac{dN_A(t)}{dt} = N_n(t)N_{A-1}(t)\langle\sigma v\rangle_{A-1} - N_n(t)N_A(t)\langle\sigma v\rangle_A - \lambda_\beta(t)N_A(t)$$

where  $N_n(t)$  is the neutron density at time  $t$  and  $\lambda_\beta$  is the  $\beta$  decay rate. Clearly this is one of a couple set of equations, complicated to solve in that the initial conditions would have to be fully specified, and the time evolution of  $N_n$  given. The equation allows for destruction of mass number  $A$  by either neutron capture or  $\beta$  decay, but the usual case is that the  $\beta$  decay dominates if that channel is open, and otherwise the neutron capture occurs. If we take the later case and envision a constant neutron exposure, so that it makes sense to define an average cross section

$$\langle\sigma v\rangle = \sigma_A\langle v\rangle$$

over the Maxwell-Boltzmann distribution of relative velocities, then

$$\frac{dN_A(t)}{dt} = \langle v \rangle N_n(t) (\sigma_{A-1} N_{A-1} - \sigma_A N_A)$$

If equilibrium has been achieved in the mass flow the LHS is zero and

$$\frac{N_A}{N_{A-1}} = \frac{\sigma_{A-1}}{\sigma_A}$$

That is, the abundance achieved is inversely proportional to the neutron cross section: if the capture rate is slow, then mass piles up at that target number. Of course, the same argument goes through if  $\beta$  decay is the destruction channel (and the  $\beta$  decay rate is presumably fast). The low neutron capture cross sections at the closed shells should result in mass peaks, just as observation shows. It also follows that equilibrium will set in most quickly in the broad plateaus between the mass peaks: mass must pile up at the closed shells before the closed shell is breached. Thus if the neutron flux is prematurely ended, the synthesis may not have yet gone beyond, for example, the  $N \sim 82$  peak.

In fact, if equilibrium were always reached over the entire range of the isotopes, then all the abundances would be in a proportion that tracks the inverse of their neutron capture cross sections. This is not what is observed: there is a drop in the abundance beyond each mass peak. Careful investigations indicate the s-process distribution observed in nature is the result of a series of neutron exposures, e.g., total neutron fluences

$$\tau = \int_0^t \langle v \rangle N_n(t) dt$$

This has units of  $\text{cm}^{-2}$ , that is, of flux times time. In fact, it has been concluded that two types of exposures, one involving a smaller fluence and the second one about four times larger, are required to produce the observed distribution.

Several sites have been suggested for the s-process, but one well accepted site is in the helium-burning shell of a red giant, where temperatures are sufficiently high to liberate neutrons by the reaction  $^{22}\text{Ne}(\alpha, n)^{25}\text{Mg}$ , where the  $^{22}\text{Ne}$  is produced from helium burning on

the elements the CNO cycle left after hydrogen burning.

Finally, we note the s-process cannot proceed beyond  $^{209}\text{Bi}$ : neutron capture on this isotope leads to a decay chain that ends with  $\alpha$  emission. This is a gap the s-process cannot cross. It follows that the transuranic elements must have some other origin.

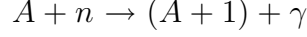
#### 5.4 The r-process

The plot of the s-process path in the  $(N,Z)$  plane, shown in the previous subsection, demonstrates that certain nuclei on the neutron-rich side of the valley of stability will be missed in the s-process. This indicates a second mechanism for synthesizing heavy nuclei is needed. More convincing evidence is shown in the figure, where the mass peaks at  $A \sim 130$  and  $A \sim 190$  are shown to split into two components, one corresponding to the expected s-process closed-neutron-shell peaks at  $N \sim 82$  and  $N \sim 126$ , and the second shifted to lower  $N$ ,  $\sim 76$  and  $\sim 116$ .

This second process is the r- or rapid-process, characterized by:

- The neutron capture is fast compared to  $\beta$  decay rates.
- Thus the equilibrium maintained in  $(n, \gamma) \leftrightarrow (\gamma, n)$ : neutron capture fills up the available bound levels in the nucleus until this equilibrium sets in. The new Fermi level depends on the temperature and the relative  $n/\gamma$  abundance.
- The nucleosynthesis rate is thus controlled by the  $\beta$  decay rate: each  $\beta^-$  capture converting  $n \rightarrow p$  opens up a hole in the neutron Fermi sea allowing another neutron to be captured.
- The nucleosynthesis path is along exotic, neutron-rich nuclei that would be highly unstable under normal laboratory conditions.
- In analogy with the s-process calculation we did (where the production and destruction of a given isotope depended on the rate-controlling production and destruction neutron-capture cross sections  $\sigma_{A-1}$  and  $\sigma_A$ ), the r-process abundance  $A(Z,N) \propto [\omega_\beta(Z,N)]^{-1}$  (the new rate-controlling reaction) for constant neutron exposure and equilibrated mass flow.

Let's first explore the  $(n, \gamma) \leftrightarrow (\gamma, n)$  equilibrium condition, which requires that the rate for  $(n, \gamma)$  balances that for  $(\gamma, n)$  for an average nucleus. So consider the formation cross section



This is an exothermic reaction, as the neutron drops into the nuclear well. Our averaged cross section, assuming a resonant reaction (the level density is high in heavy nuclei) is

$$\langle \sigma v \rangle_{(n, \gamma)} = \left( \frac{2\pi}{\mu k T} \right)^{3/2} \frac{\Gamma_n \Gamma_\gamma}{\Gamma} e^{-E/KT}$$

where  $E \sim 0$  is the resonance energy. Thus the rate is

$$r_{(n, \gamma)} \sim N_n N_A \left( \frac{2\pi}{\mu k T} \right)^{3/2} \frac{\Gamma_n \Gamma_\gamma}{\Gamma}$$

This has to be compared to the  $(\gamma, n)$  rate.

The  $(\gamma, n)$  reaction requires the photon number density in our gas. This is the Bose Einstein

$$N(\epsilon) = \frac{8\pi}{c^3 h^3} \frac{\epsilon^2 d\epsilon}{e^{\epsilon/kT} - 1}$$

The high-energy tail of the normalized distribution can thus be written

$$\sim \frac{1}{N_\gamma \pi^2} \epsilon^2 e^{-\epsilon/kT} d\epsilon$$

Although we will not be needing it, the approximate expression for the total photon density (gotten by integrating the distribution over all energies) is

$$N_\gamma \sim \frac{\pi}{13} (kT)^3$$

In the two expressions above we have set  $\hbar = c = 1$ .

Now we need the resonant cross section in the  $(\gamma, n)$  direction. For photons the wave number is proportional to the energy, so

$$\sigma_{(\gamma,n)} = \frac{\pi}{\epsilon^2} \frac{\Gamma_\gamma \Gamma_n}{(\epsilon - E_r)^2 + (\Gamma/2)^2}$$

As the velocity is  $c=1$ ,

$$\langle \sigma v \rangle = \frac{1}{\pi^2 N_\gamma} \int_0^\infty \epsilon^2 e^{-\epsilon/kT} d\epsilon \frac{\pi}{\epsilon^2} \frac{\Gamma_\gamma \Gamma_n}{(\epsilon - E_r)^2 + (\Gamma/2)^2}$$

We evaluate this in the usual way for a sharp resonance, remember that the energy integral over just the denominator above (the sharply varying part) is  $2\pi/\Gamma$ :

$$\sim \frac{\Gamma_\gamma \Gamma_n}{N_\gamma} e^{-E_r/kT} \frac{2}{\Gamma}$$

So that the rate becomes

$$r_{(\gamma,n)} \sim 2N_{A+1} \frac{\Gamma_\gamma \Gamma_n}{\Gamma} e^{-E_r/kT}$$

Equating the  $(n, \gamma)$  and  $(\gamma, n)$  rates and taking  $N_A \sim N_{A-1}$  then yields

$$N_n \sim \frac{2}{(\hbar c)^3} \left( \frac{\mu c^2 kT}{2\pi} \right)^{3/2} e^{-E_r/kT}$$

where the  $\hbar$ s and  $c$ s have been properly inserted to give the right dimensions. Now  $E_r$  is essentially the binding energy. So plugging in the conditions  $N_n \sim 3 \times 10^{23}/\text{cm}^3$  and  $T_9 \sim 1$ , we find that the binding energy is  $\sim 2.4$  MeV. Thus neutrons are bound by about 30 times  $kT$ , a value that is still small compared to a typical binding of 8 MeV for a normal nucleus. (In this calculation I calculated the neutron reduced mass assuming a nuclear target with  $A=150$ .)

Now I should stress that here, as before in these lectures, I have neglected the spins of the particles. This clearly comes in because, when one uses the distribution for photons mentioned earlier, the two helicity states of the photon have been counted. Thus we should have carefully averaged over initial photon spins, etc., in doing our cross sections. Our earlier work on  $(p, \gamma)$  and other reactions had the same defects. Thus don't take factors of 2 seriously. Also note that the derivation done above can be run through for any other reaction, like  $(\alpha, \gamma)$ , which is needed in the home work.

We mentioned before that gaps existed at the shell closures, at  $N \sim 82$  and  $126$ . When a shell gap is reached in the r-process (I'll illustrate this on the board), the neutron number of the nucleus remains fixed until the nucleus can change sufficiently to overcome the gap, i.e., bring another bound neutron quantum level below the continuum. Thus  $N$  remains fixed while successive  $\beta$  decays occur. In the  $(N,Z)$  trajectory, the path is along increasing  $Z$  with fixed  $N$ : every  $\beta$  decay is followed by an  $(n, \gamma)$  reaction to fill the open neutron hole, but no further neutrons can be captured until the gap is overcome.

The path of the r-process is shown in the accompanying figure. The closed neutron shells are called the waiting points, because it takes along time for the successive  $\beta$  decays to occur to allow progression through higher  $N$  nuclei. The  $\beta$  decays are slow at the shell closures. Just as in the s-process, the abundance of a given isotope is inversely proportional to the  $\beta$  decay lifetime. Thus mass builds up at the waiting points, forming the large abundance peaks seen in the figure.

After the r-process finishes (the neutron exposure ends) the nuclei decay back to the valley of stability by  $\beta$  decay. This can involve some neutron spallation ( $\beta$ -delayed neutrons) that shift the mass number  $A$  to a lower value. But it certainly involves conversion of neutrons into protons, and that shifts the r-process peaks at  $N \sim 82$  and  $126$  to a lower  $N$ , off course. This effect is clearly seen in the abundance distribution: the r-process peaks are shifted to lower  $N$  relative to the s-process peaks.

It is believed that the r-process can proceed to very heavy nuclei ( $A \sim 270$ ) where it is finally ended by  $\beta$ -delayed and n-induced fission, which feeds matter back into the process at an  $A \sim A_{max}/2$ . Thus there may be important cycling effects in the upper half of the r-process distribution.

What is the site(s) of the r-process? This has been debated many years and still remains a

controversial subject.

- The r-process requires exceptionally explosive conditions

$$\rho(n) \sim 10^{20} \text{ cm}^{-3} \quad T \sim 10^9 \text{ K} \quad t \sim 1 \text{ sec}$$

- both primary and secondary sites proposed

primary: requiring no preexisting metals

secondary: neutron capture occurs on s-process seeds

⇔ different evolution with galactic metallicity

- suggested primary sites:

- 1) neutronized atmosphere above proto-neutron star in a Type II supernova
- 2) neutron-rich jets from supernovae or neutron star mergers
- 3) inhomogeneous big bangs

⋮

- secondary sites (where  $\rho(n)$  can be lower)

- 1) He/C zones in Type II supernovae
- 2) red giant He flash
- 3)  $\nu$  spallation neutrons in He zone

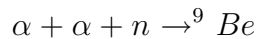
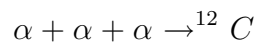
⋮

The balance of evidence favors a primary site, so one requiring no preenrichment of heavy s-process metals. Among the evidence:

1) HST studies of very-metal-poor halo stars: The most important evidence are the recent HST measurements of Sneden et al. of very metal-poor stars ( $[\text{Fe}/\text{H}] \sim -1.7$  to  $-3.12$ ) where an r-process distribution very much like that of our sun has been seen for  $Z \gtrsim 56$ . Furthermore, in these stars the iron content is variable. This suggests that the "time resolution" inherent in these old stars is short compared to galactic mixing times (otherwise Fe would be more constant). The conclusion is that the r-process material in these stars is most likely from one or a few local supernovae. The fact that the distribution matches the solar

r-process (at least above charge 56) strongly suggests that there is some kind of unique site for the r-process: the solar r-process distribution did not come from averaging over many different kinds of r-process events. Clearly the fact that these old stars are enriched in r-process metals also strongly argues for a primary process: the r-process works quite well in an environment where there is little initial s-process metals.

2) There are also fairly good theoretical arguments that a primary r-process occurring in a core-collapse supernova might be viable. First, galactic chemical evolution studies indicate that the growth of r-process elements in the galaxy is consistent with low-mass Type II supernovae in rate and distribution. More convincing is the fact that modelers have shown that the conditions needed for a r-process (very high neutron densities, temperatures of 1-3 billion degrees) might be realized in a supernova. The site is the last material blown off the supernova, the material just above the mass cut. When this material is blown off the star initially, it is a very hot neutron-rich, radiation-dominated gas containing neutrons and protons, but an excess of the neutrons. As it expands off the star and cools, the material first goes through a freezeout to  $\alpha$  particles, a step that essentially locks up all the protons in this way. Then the  $\alpha$ s interact through reactions like



to start forming heavier nuclei. Note, unlike the big bang, that the density is high enough to allow such three-body interactions to bridge the mass gaps at  $A = 5,8$ . The  $\alpha$  capture continues up to heavy nuclei, to  $A \sim 80-100$ , in the network calculations. This was a surprising results of the network calculations that were performed. The net result is a small number of "seed" nuclei, a lot of  $\alpha$ s, and left over excess neutrons. These neutrons preferentially capture on the heavy seeds to produce an r-process. Of course, what is necessary is to have  $\sim 100$  excess neutrons per seed in order to successfully synthesis heavy mass nuclei. Some

of the modelers find conditions where this almost happens.

There are some very nice aspects of this site: the amount of matter ejected is about  $10^{-5} - 10^{-6}$  solar masses, which is just about what is needed over the lifetime of the galaxy to give the integrated r-process metals we see, taking a reasonable supernova rate. But there are also a few problems:

- The calculated entropies, neutron fractions are a bit too low to produce a successful  $A \sim 190$  peak.
- $^{129}I/^{127}I$ ,  $^{182}Hf/^{180}Hf$  chronometers argue for two distinct types of r-process events, with the  $A \sim 130$  associated with rarer, larger events and the  $A \sim 190$  with more frequent, smaller events. It has been suggested that these might be supernovae leading to neutron stars vs. those leading to black holes, respectively.

There are some interesting neutrino physics issues that I'll mention briefly which depend on the characteristics of the supernova (or "hot bubble") r-process:

$$\begin{aligned} \text{r-process T: } & 3 \cdot 10^9 \text{K} \rightarrow 1 \cdot 10^9 \text{K} \\ \text{freezeout radius } & \sim 600\text{-}1000 \text{ km} \\ L_\nu & \sim (0.015\text{-}0.005) \cdot 10^{51} \text{ ergs}/(100\text{km})^2 \text{s} \\ \tau & \sim 3 \text{ sec} \end{aligned}$$

Thus the neutrino fluence after freezeout (when the temperature has dropped below  $10^9\text{K}$  and the r-process stops) is  $\sim (0.045\text{-}0.015) \cdot 10^{51} \text{ ergs}/(100\text{km})^2 \Rightarrow$

the ejection of r-process material occurs  
in an intense neutrino flux

This brings up the question of whether the neutrino flux could have any effect on the r-process. This is actually a more general issue about a nucleosynthesis mechanism called the neutrino process that we will now discuss.

## 5.5. The Neutrino Process

We have just argued that core-collapse supernovae are one of the major engines driving galactic chemical evolution, producing some of the most abundant metals (C, O, Ne) in hydrostatic evolution; producing many others in explosive burning; and creating many of the heavy elements (most likely) through the r-process. I now want to turn to a topic of some personal interest, the subtler but nevertheless interesting synthesis that can be associated directly with the enormous neutrino fluxes produced by supernovae.

One of the problems - still controversial - that may be connected with the neutrino process is the origin of the light elements Be, B and most of Li, which aren't produced in sufficient amounts in the big bang or in any of the stellar mechanisms we have discussed. The traditional explanation has been cosmic ray spallation interactions with C, O, and N in the interstellar medium. In this picture, cosmic ray protons collide with C at relatively high energy, knocking the nucleus apart. So in the debris one can find nuclei like  $^{10}\text{B}$ ,  $^{11}\text{B}$ , and  $^7\text{Li}$ .

But there are some problems with this picture. First of all, this is an example of a secondary mechanism: the interstellar medium must be enriched in the C, O, and N to provide the targets for these reactions. Thus cosmic ray spallation must become more effective as the galaxy ages. That is, the abundance of  $^{11}\text{B}$ , for example, would tend to grow quadratically with metallicity, since the rate of production goes linearly with metallicity. But, as one sees from the diagram, it is almost perfectly linear.

A second problem is that the spectrum of cosmic ray protons is energetic, leading to roughly comparable production of the two isotopes  $^{10}\text{B}$  and  $^{11}\text{B}$ . That is, while it takes more energy to knock two nucleons out of carbon than one, this difference is not significant compared to typical cosmic ray energies. (More about cosmic rays later.) More careful arguments lead to the expectation that the abundance ratio of  $^{11}\text{B}$  to  $^{10}\text{B}$  might be  $\sim 2$ . In nature, it is

greater than 4.

Fans of cosmic ray spallation have offered solutions to this problem, e.g., similar reactions occurring in the atmospheres of nebulae involving lower energy cosmic rays. But I want to focus on an alternative explanation here.

Before we get to the main issue, a point of nuclear physics. Previously we spoke about weak interactions in nuclei involving the Gamow-Teller (spin-flip) and Fermi operators. These are the appropriate operators when one probes the nucleus at a wavelength - that is, at a size scale - where the nucleus responds like an elementary particle. That is, we can characterize its response by its macroscopic quantum numbers, the spin and charge. On the other hand, the nucleus is a composite object and, therefore, if it is probed at shorter length scales, all kinds of interesting radial excitations will result, analogous to the vibrations of a drumhead. For a reaction like neutrino scattering off a nucleus, the full operator involves the additional factor

$$e^{i\vec{k}\cdot\vec{r}} \sim 1 + i\vec{k} \cdot \vec{r}$$

where the expression on the right is valid if the magnitude of  $\vec{k}$  is not too large. Thus the full charge operator includes a “first forbidden” term

$$\sum_{i=1}^A \vec{r}_i \tau_3(i)$$

and similarly for the spin operator

$$\sum_{i=1}^A [\vec{r}_i \otimes \vec{\sigma}(i)]_{J=0,1,2} \tau_3(i)$$

These operators generate collective radial excitations, leading to the so-called “giant resonance” excitations in nuclei. The giant resonances are typically at an excitation energy of 20-25 MeV in light nuclei. One important property is that these operators satisfy a sum rule (Thomas-Reiche-Kuhn) of the form

$$\sum_f |\langle f | \sum_{i=1}^A r(i) \tau_3(i) | i \rangle|^2 \sim \frac{NZ}{A} \sim \frac{A}{4}$$

where the sum extends over a complete set of final nuclear states. These first-forbidden operators tend to dominate the cross sections for scattering the high energy supernova neutrinos ( $\nu_\mu$ s and  $\nu_\tau$ s), with  $E_\nu \sim 25$  MeV, off light nuclei. From the sum rule above, it follows that the cross sections per target *nucleon* are roughly constant.

The simplest example of the neutrino process involves the Ne shell in a supernova. Because of the first-forbidden contributions, the cross section for inelastic neutrino scattering to the giant resonances in Ne is  $\sim 3 \cdot 10^{-41}$  cm<sup>2</sup>/flavor. So this is the reaction

$$\nu + A \rightarrow \nu' + A^* \quad \Delta E \sim 20\text{MeV}$$

where the 20 MeV is the excitation energy of Ne after the scattering. Now a supernova releases about  $3 \times 10^{53}$  ergs in neutrinos, which converts to about  $4 \times 10^{57}$  heavy flavor neutrinos. The Ne shell in a  $20 M_\odot$  star has at a radius  $\sim 20,000$  km. Thus the neutrino fluence through the Ne shell is

$$\phi \sim \frac{4 \cdot 10^{57}}{4\pi(20,000\text{km})^2} \sim 10^{38}/\text{cm}^2$$

Thus folding the fluence and cross section,

$$\Rightarrow \frac{1}{300} \text{ of the nuclei interact}$$

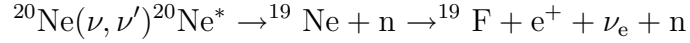
This is quite interesting since the astrophysical origin of <sup>19</sup>F had not been understood. This, the only stable isotope of fluorine, has an abundance

$$\frac{{}^{19}\text{F}}{{}^{20}\text{Ne}} \sim \frac{1}{3100}$$

We will now show that the <sup>19</sup>F in your toothpaste was created by neutral current neutrino reactions deep inside some ancient supernova.

The calculation goes as follows:

- The  $^{20}\text{Ne}$  shell resides at  $(1-3) \cdot 10^4$  km in a  $25 M_{\odot}$  evolved, presupernova star
- When Ne is excited by  $\sim 20$  MeV through inelastic neutrino scattering, it breaks up in two ways

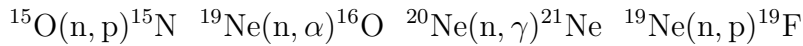


with the first reaction occurring about 1/3 the time and the second 2/3 of the time. Both reactions produce fluorine. Thus we conclude that neutral current neutrino reactions create an instantaneous abundance ratio in the Ne shell of

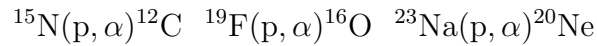
$$\frac{^{19}\text{F}}{^{20}\text{Ne}} \sim \frac{1}{300}$$

which is larger than observed.

- This raises the issue of whether the produced  $^{19}\text{F}$  survives. In the first  $10^{-8}$  sec the coproduced neutrons in the first reaction react via

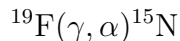


with the result that about 70% of the  $^{19}\text{F}$  produced via spallation of neutrons is then immediately destroyed, primarily by the  $(\text{n}, \alpha)$  reaction above. In the next  $10^{-6}$  sec the coproduced protons are also processed



with the latter two reactions competing as the primary proton poisons. This makes an important prediction: stars with high Na abundances should make more F, as the  $^{23}\text{Na}$  acts as a proton poison to preserve the produced F.

- Finally, there is one other destruction mechanism, the heating associated with the passage of the shock wave. It turns out that the F produced prior to shock wave passage can survive if it is in the outside half of the Ne shell. The reaction



destroys F for peak explosion temperatures exceeding  $1.7 \cdot 10^9\text{K}$ . Such a temperature is produced at the inner edge of the Ne shell by the shock wave heating, but not at the outer edge.

If all of this physics is handled is a careful network code that include the shock wave heating and F production both before and after shock wave passage, the following are the results:

$[{}^{19}\text{F}/{}^{20}\text{Ne}]/[{}^{19}\text{F}/{}^{20}\text{Ne}]_{\odot}$	$T_{\text{heavy } \nu}(\text{MeV})$
0.14	4
0.6	6
1.2	8
1.1	10
1.1	12

One sees that the attribution of F to the neutrino process argues that the heavy flavor  $\nu$  temperature must be greater than 6 MeV, a result theory favors. One also sees that F cannot be overproduced by this mechanism: although the instantaneous production of F continues to grow rapidly with the neutrino temperature, too much F results in its destruction through the  $(p, \alpha)$  reaction, given a solar abundance of the competing proton poison  ${}^{23}\text{Na}$ . Indeed, this illustrates an odd quirk: although in most cases the neutrino process is a primary mechanism, one needs  ${}^{23}\text{Na}$  present to produce significant F. Thus in this case the neutrino process is a secondary mechanism.

While there are other significant neutrino process products ( ${}^7\text{Li}$ ,  ${}^{138}\text{La}$ ,  ${}^{180}\text{Ta}$ ,  ${}^{15}\text{N}$  ...), the most important product is  ${}^{11}\text{B}$ , produced by spallation off carbon. A calculation by Timmes et al. found that the combination of the neutrino process, cosmic ray spallation and big-bang nucleosynthesis together can explain the evolution of the light elements. The neutrino process, which produces a great deal of  ${}^{11}\text{B}$  but relatively little  ${}^{10}\text{B}$ , combines with the cosmic ray spallation mechanism to yield the observed isotope ratio. Again, one prediction of

this picture is that early stars should be  $^{11}\text{B}$  rich, as the neutrino process is primary and operates early in our galaxy's history; the cosmic ray production of  $^{10}\text{B}$  is more recent. The figure shows the evolution of boron relative to hydrogen as a function of the metallicity  $[\text{Fe}/\text{H}]$ . The solid line shows the calculated boron abundance, with the dashed lines showing a factor-of-two variation. This is compared to various abundance determinations, showing good agreement. This is another example where HST studies of metal-poor stars are providing important tests of models of stellar nucleosynthesis.

There is hope that such studies will soon be able to discriminate between  $^{10}\text{B}$  and  $^{11}\text{B}$ : as yet this has not been done.

## 5.6 The Neutrino Process and the r-process

Now it may have occurred to you that we earlier discussed another process occurring in a supernova that could conceivably be affected by the neutrinos: the r-process. One fascinating branch of this discussion involves the neutrino reactions in the neutron-rich soup in which the hot bubble r-process is thought to occur: neutrino oscillations of the form

$$\nu_e \leftrightarrow \nu_\tau$$

can lead to an anomalously hot  $\nu_e$  spectrum which, via the reaction

$$\nu_e + n \rightarrow e^- + p$$

then converts the soup into one that is proton rich, thereby destroying an essential requirement for the r-process. With the assumption that the hot bubble is the correct r-process site, one can then rule out a number of interesting neutrino oscillation scenarios. This is quite an active area for research.

Here we will examine the less exotic effects associated with standard model neutrino interactions. The hot bubble r-process occurs *much* closer to the star than our Ne radius of 20,000

km: estimates are 600-1000 km. The r-process is completed in about 10 seconds (when the temperature drops to about one billion degrees), but the neutrino flux is still significant as the r-process freezes out. The net result is that the “post-processing” neutrino fluence - the fluence that can alter the nuclear distribution after the r-process is completed - is about 100 times larger than that responsible for fluorine production in the Ne zone. Recalling that 1/300 of the nuclei in the Ne zone interacted with neutrinos, and remembering that the relevant neutrino-nucleus cross sections scale as  $A$ , one quickly sees that the probability of a r-process nucleus interacting with the neutrino flux is approximately unity.

Because the hydrodynamic conditions of the r-process are highly uncertain, one way to attack this problem is to work backward in time. We know the final r-process distribution (what nature gives us) and we can calculate neutrino-nucleus interactions relatively well. Thus from the observed r-process distribution (including neutrino postprocessing) we can work backward to find out what the r-process distribution looked like at the point of freeze-out. In the two figures, the “real” r-process distribution - that produced at freezeout - is given by the solid lines, while the dashed lines show the effects of the neutrino postprocessing for a particular choice of fluence.

One important aspect of the figures is that the mass shift is significant. This has to do with the fact that a 20 MeV excitation of a neutron-rich nucleus allows multiple neutrons ( $\sim 5$ ) to be emitted. (Remember we found that the binding energy of the last neutron in an r-process neutron-rich nuclei was about 2 MeV under typical r-process conditions.) The second thing to notice is that the relative contribution of the neutrino process is particularly important in the “valleys” beneath the mass peaks: the reason is that the parents on the mass peak are abundant, and the valley daughters rare. In fact, it follows from this that the neutrino process effects can be dominant for precisely seven isotopes (Te, Re, etc.) lying in these valleys. Furthermore if an appropriate neutrino fluence is picked, these isotope abundances are produced perfectly (given the abundance errors). The fluences are

$$N = 82 \text{ peak} \quad 0.031 \cdot 10^{51} \text{ergs}/(100\text{km})^2/\text{flavor}$$

$$N = 126 \text{ peak} \quad 0.015 \cdot 10^{51} \text{ergs}/(100\text{km})^2/\text{flavor}$$

values in fine agreement with those that would be found in a hot bubble r-process. So this is circumstantial but significant evidence that the material near the mass cut of a type II supernova is the site of the r-process: there is a neutrino fingerprint.